Veuve, N., Dalil Safaei, S., and Smith, I.F.C. (2015). Deployment of a Tensegrity Footbridge. *Journal of Structural Engineering*, 141(11), 04015021 http://cedb.asce.org Copyright ASCE

Deployment of a tensegrity footbridge

Nicolas Veuve[1], Seif Dalil Safaei[2], Ian F.C Smith[3]

Abstract

Deployable structures are structures that transform their shape from a compact state to an extended in-service position. Structures composed of tension elements that surround compression elements in equilibrium are called tensegrity structures. Tensegrities are good candidates for deployable structures since shape transformations occur by changing lengths of elements at low energy costs. Although the tensegrity concept was first introduced in 1948, few full-scale tensegrity-based structures have been built. Previous work has demonstrated that a tensegrity-ring topology is potentially a viable system for a deployable footbridge. This paper describes a study of a near-full-scale deployable tensegrity footbridge. The study has been carried out both numerically and experimentally. The deployment of two modules (one half of the footbridge) is achieved through changing the length of five active cables. Deployment is aided by energy stored in low stiffness spring elements. Self-weight significantly influences deployment, and deployment is not reproducible using the same sequence of cable-length changes. Active control is thus required for accurate positioning of front nodes in order to complete deployment through joining both sides at center span. Additionally, testing and numerical analyses have revealed that the deployment behavior of the structure is non-linear with respect to cable-length changes. Finally, modelling the behavior of the structure cannot be done accurately using friction-free and dimensionless joints. Similar deployable tensegrity structures of class two and higher are expected to require simulation models that include joint dimensions for accurate prediction of nodal positions.

Introduction

Tensegrity structures are structures composed of tension elements (strings, tendons or cables) surrounding compression elements (bars or struts) in equilibrium (Motro et al. 2003). Various definitions of tensegrity structures exist; a concise definition has been proposed by Skelton et al. (2001) who defined a class K tensegrity structure as a stable equilibrium of axially loaded elements, with a maximum of K compressive members at the nodes.

[1]Phd Student, Applied Computing and Mechanics Laboratory, School of Architecture, Civil and Environmental Engineering (ENAC), Swiss Federal Institute of Technology (EPFL), Lausanne, Switzerland (corresponding author). Email: nicolas.veuve@epfl.ch

[2]Postdoctoral Researcher, Applied Computing and Mechanics Laboratory, School of Architecture, Civil and Environmental Engineering (ENAC), Swiss Federal Institute of Technology (EPFL), Lausanne, Switzerland.

[3]F.ASCE Professor, Applied Computing and Mechanics Laboratory, School of Architecture, Civil and Environmental Engineering (ENAC), Swiss Federal Institute of Technology (EPFL), Lausanne, Switzerland.

Tensegrity structures are identified by the number of infinitesimal mechanisms and states of self-stress (Pellegrino et al. 1986). Pellegrino et al. (1986) introduced a method for computing the number of infinitesimal mechanisms and self-stress states by singular value decomposition (SVD) of the equilibrium matrix. The design process of tensegrity structures includes simultaneous identification of geometry, topology, element axial stiffness, actuator position, and self-stressed state. Tibert and Pellegrino (2003) reviewed form-finding methods. Several studies have included the derivation of tangent stiffness matrix for a pre-stressed framework (Argyris and Scharpf 1972, Murakami 2001 and Guest 2006). Skelton et al. (2014) proposed a topology optimization method for minimum mass design of tensegrity bridges and showed that the optimized design has a multi-scale character.

Tensegrities are attractive for deployment and active control since their shape can be changed through changing lengths of elements. In addition to carrying loading, the elements in tensegrity structures can be actuators and sensors (Skelton et al. 2001).

In several studies, e.g. (Furuya. 1992, Tibert. 2002, Furuya et al. 2006, Dalil Safaei et al. 2013), tensegrities have been proposed as deployable booms for space missions. Zolesi et al. (2012) successfully demonstrated deployment repeatability of a large tensegrity reflector antenna through a 1/4 scale prototype equipped with a gravity compensation system.

Tensegrities are good candidate for active structures since they can change their shape under changing environments, such as new loading situations. Fest et al. (2004) employed telescopic struts to investigate the active control behavior of a five-module tensegrity structure. In several studies, biomimetic properties of active tensegrity structures have been studied (Adam and Smith 2008; Domer 2003; Domer and Smith 2005). These structures were not deployable.

Although studies have been carried out on deployment of tensegrity structures, very few near full-scale deployable tensegrity structures have been built. Physical models are important for exploration, validation and development of ideas. In addition, a physical model should be large enough to be able to study important full-scale challenges.

The influence of joint characteristics on deployment of tensegrity structures has not been studied. This is particularly important for structures of class 2 and higher since a pre-defined sequence of length changes of active cables may not result in a successful deployment due to joint configuration and friction effects. In addition, no study has been performed to investigate the influence of self-weight on deployment.

This paper studies the deployment of a clustered-cable-spring tensegrity configuration that was adapted from a design proposal by Motro et.al (2006). Clustered cables are continuous cables that slide continuously over joints located at the ends of struts. Design and analysis of tensegrity footbridges have been studied by several researchers. Tensegrity-ring modules were introduced by Pugh (1976). These modules were studied for deployment and named ring modules by Motro et.al (2006) because of their hollow interior space. Nguyen (2011) and Cevaer et al. (2012)

studied the structural behavior of a single pentagonal ring module under the assumption that there was no cable continuity. A near full-scale tensegrity footbridge has been built to study strategies for deployment. More specifically, objectives of this paper are as follows:

- Describe an experimental study of a clustered-cable-spring configuration for deployment of a near-full-scale tensegrity footbridge.
- Demonstrate the need for active control for reproducible deployment behavior.
- Evaluate the assumption of dimensionless joints for prediction of deployment behavior.
- Study the influence of self-weight on deployment.

The next sections provide details, results and evaluations related to these goals.

The tensegrity ring footbridge

The footbridge is composed of four identical pentagonal ring modules connected together in a "hollow-rope" system (Rhode-Barbarigos et al. 2010, Bel Hadj Ali et al 2010, and Motro et.al 2006). Each pentagonal ring module in Figure 1 has 15 struts and 30 cables. Tensegrity structures are characterized by the number of self-stress states and infinitesimal mechanisms. Analysis of the equilibrium matrix reveals no infinitesimal mechanisms and six independent states of self-stress. Each tensegrity ring module is a class two tensegrity structure (Skelton et al. 2001). The empty space in the tensegrity ring module is employed for footbridge pedestrian traffic.

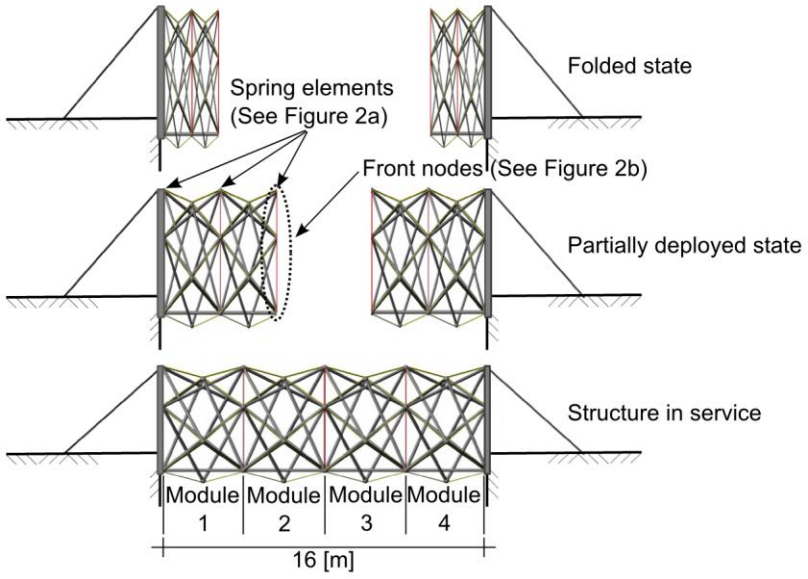

Figure 1: Deployment illustration of four-module tensegrity footbridge. This paper studies the deployment of one half of a ¼ scale model of the footbridge (adapted from Rhode-Barbarigos et al. (2010) and Rhode-Barbarigos et al. (2012b))

Rhode-Barbarigos et al. (2010) and Bel Hadj Ali et al. (2010) studied the serviceability of a 16 m span and 6.2 m diameter tensegrity footbridge without considering clustered cables and

deployability. Rhode-Barbarigos et al. (2012b) then studied several deployment methods and showed that utilizing springs, inspired from (Schenk et al. 2007), and clustered-cables reduces the number of actuators required for controlled deployment. Bel Hadj Ali et al. (2011) proposed an analysis method for clustered tensegrity structures through a modified dynamic relaxation algorithm. Clustered cable elements run continuously through nodes. They influence the mechanics of tensegrity structures through reducing number of kinematic constraints and changing the internal-force distribution of the elements (Moored and Bart-Smith 2009).

A 1/4 scale model has been designed, manufactured and assembled in order to study deployment behavior (Figure 2). Each half is composed of 15 springs, 5 continuous cables, 30 struts and 20 cables. Also, each half is controlled by five continuous active cables. Each active continuous cable starts from a node connected to the support and ends at the front nodes. Figure 2 shows continuous actuated cables (active cables) and spring elements. Active cables are connected to the front nodes of the half bridge (Figure 1). The length of each active cable is changed through winding or unwinding the cable on a drum that is fixed on moving support (Figure 3). An actuation step or a control command is the length changes of the five active cables applied during one step of deployment.

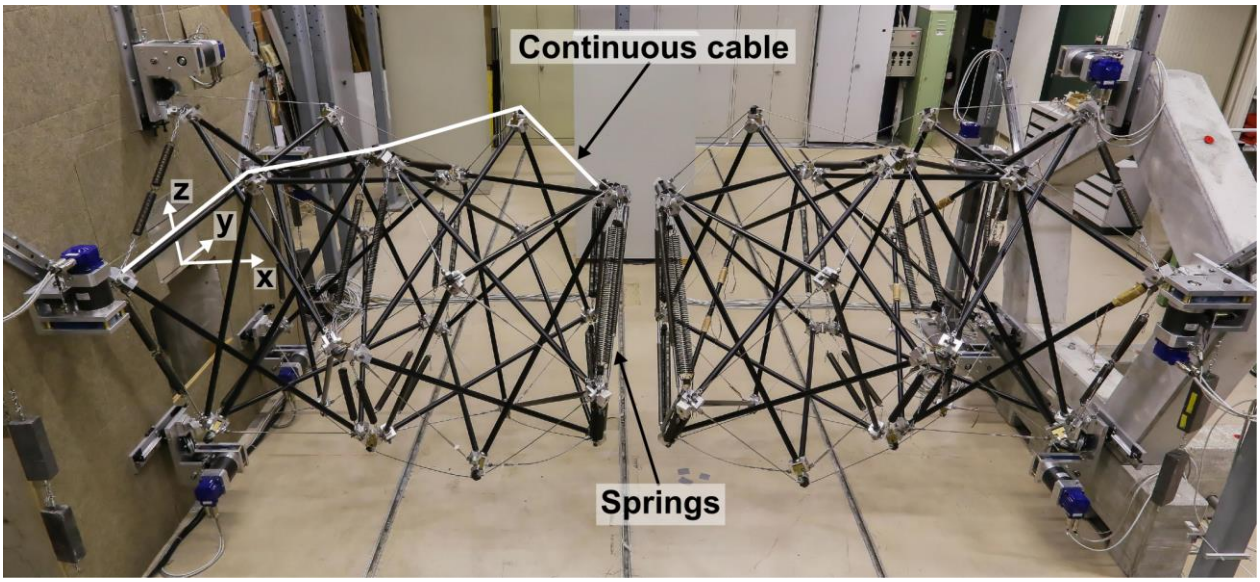

Figure 2: (a) Side view of the near-full scale tensegrity footbridge

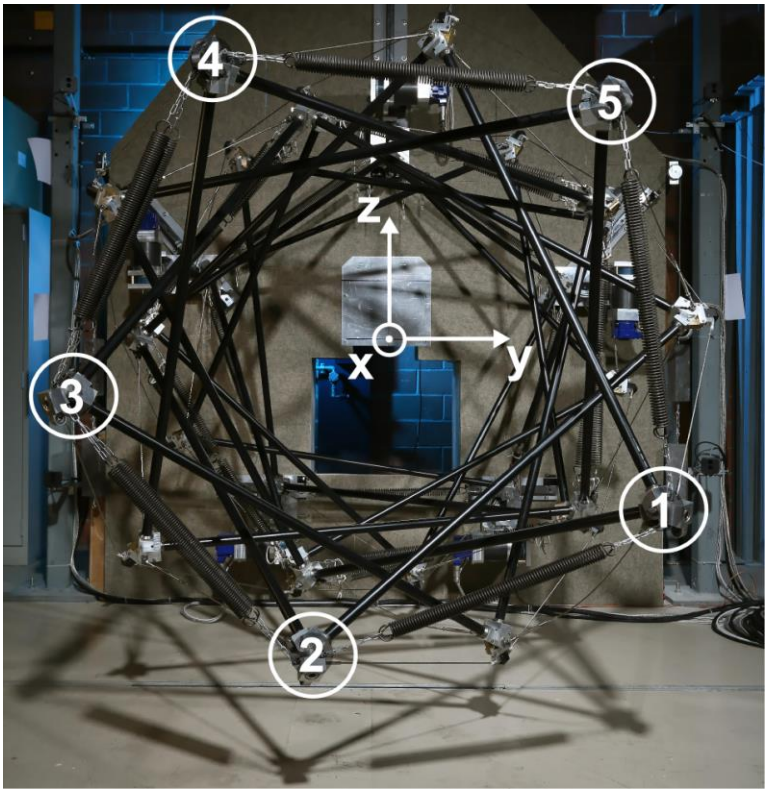

Figure 2: (b) front view with node numbering of the near-full scale tensegrity footbridge

The structural weight of each half is approximately 100 kg. Both ends move in rail-support systems (Figure 3). Struts are made of steel hollow tube section profiles with a length of 1.35 m, a diameter of 28 mm and a thickness of 1.5 mm. The steel grade of the struts is S355 with a modulus of elasticity of 210 GPa. Cables have a diameter of 4 mm and are made of stainless steel with a modulus of elasticity of 120 GPa. The value of spring stiffnesses at the support is 2 kN/m and is 2.9 kN/m for other springs. The footbridge has 25 joints per side including 5 inter-module joints and 5 support joints. Joints are designed and built to support continuous cables. Joints are based on fork-to-fork design with additional components for continuous cables (Figure 4). Position measurement has been performed with an optical tracking system. Each half bridge has four states of self-stress.

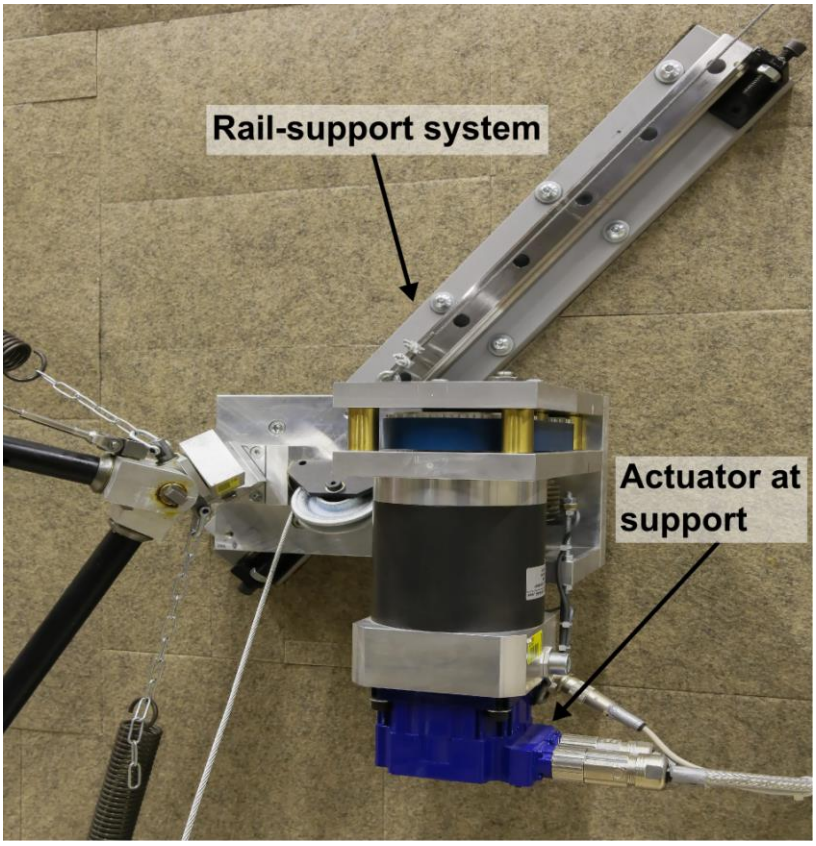

Figure 3: Support-rail system and actuator at support

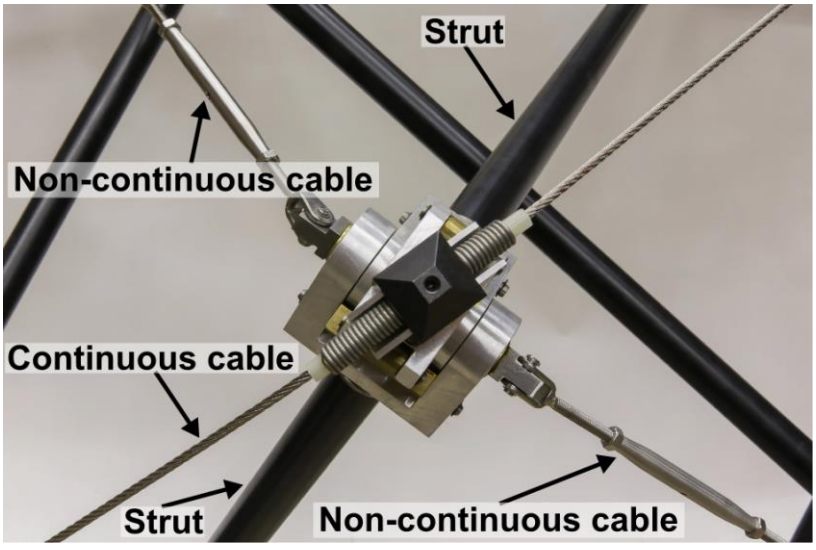

Figure 4: Joint connecting two struts with one continuous cable and two non-continuous cables

Numerical analysis

An analysis algorithm has been developed explicitly for deployment of tensegrity modules. In this study, dynamic relaxation (DR) (Barnes 1999) with kinetic damping is employed for

incremental static analysis. DR is a static analysis method based on the equation of motion, where the static solution is seen as the resulting equilibrium state of a damped vibration. DR has been used successfully for hundreds of tent structures and cable stayed bridges. Most modern analysis software packages include DR modules.

Quasi-static actuation and frictionless motion are assumed for deployment. Quasi-static actuation means that, due to slow deployment, acceleration and velocity terms in the deployment analysis are neglected. Therefore, the dynamic analysis of the deployment may be approximated by a series of static analyses. The inputs to the program are current configuration, pre-stress, axial stiffness of the elements and loading state. Self-weight is the only loading applied to the structure during deployment.

The DR algorithm was modified to take into account clustered cables and spring elements. A detailed presentation of the modified DR method can be found in (Bel Hadj Ali et al. 2011). The numerical model does not include the dimensions of joints and consequently, there are modelling challenges associated with eccentricity, friction and the effect of strut contact on deployment. Although recent work shows that a beam-type model is essential for predicting dynamic behavior of compressed members (Ashwear and Eriksson 2014), the elements of structures in this study are assumed to be bars with axial forces only since behavior is modeled to be quasi-static.

Deployment

During deployment, the shape of structure changes from a compact state to an expanded configuration. The goal is to have both halves start from a compact configurations (folded), deploy and then become connected without human interaction. An acceptable difference between desired position and real position for connection of the joints is 15 mm for a near-full-scale structure.

Deployment and folding are performed through changing the lengths of active cables. Due to the helix cable topology, the deployment motion of a hollow-rope system is composed of rotation, translation and dilation among the pentagonal faces of a prism. A deployment path can be pre-defined for both numerical and physical models. Each actuation step is defined as a set of length changes of active cables. Each new stable configuration is obtained first through numerical analysis. The length changes of active cables are not equal.

The input parameters for DR analysis are axial stiffness of elements, change of unstressed length of cables, and the initial configuration. Two types of DR analyses are conducted to compare the test results with those from experimental tests. Numerical analysis with design stresses includes the values from Rhode-Barbarigos et al. (2012b). Numerical analyses with measured cable loads are performed through introducing values that were obtained from measurements taken from the physical model. A tension measurement instrument is employed to obtain cable loads through a deformation measurement.

Experimental testing

Several spring stiffnesses were analysed. Figure 5 shows the length of structure when first strut contact occurs during folding. The structure is set at its full deployed length of 2 m. Active cables are shortened equally and simultaneously. Figure 5 shows that for low spring stiffness, the length of the structure at first strut contact is higher than for higher spring stiffness. Higher spring stiffness helps reduce the deflection of the structure by increasing the stiffness of the structure. An important conclusion is that in addition to topology, deflection (due to self-weight) is a factor that influences deployment.

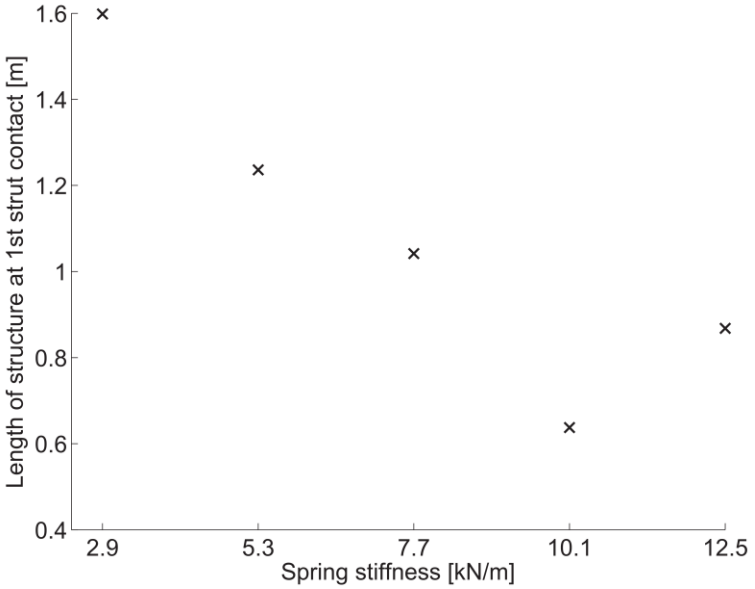

Figure 5: Structural length change due to different values of spring stiffness.

Figure 6 shows the relative change of position for node 4 over 10 cycles of folding and deployment. The cycles are performed with equal length changes of all active cables. The length change of active cables for each stage of folding and deployment is ± 0.215 m. Measurements are taken at 3 points on the horizontal deployment axis (x).

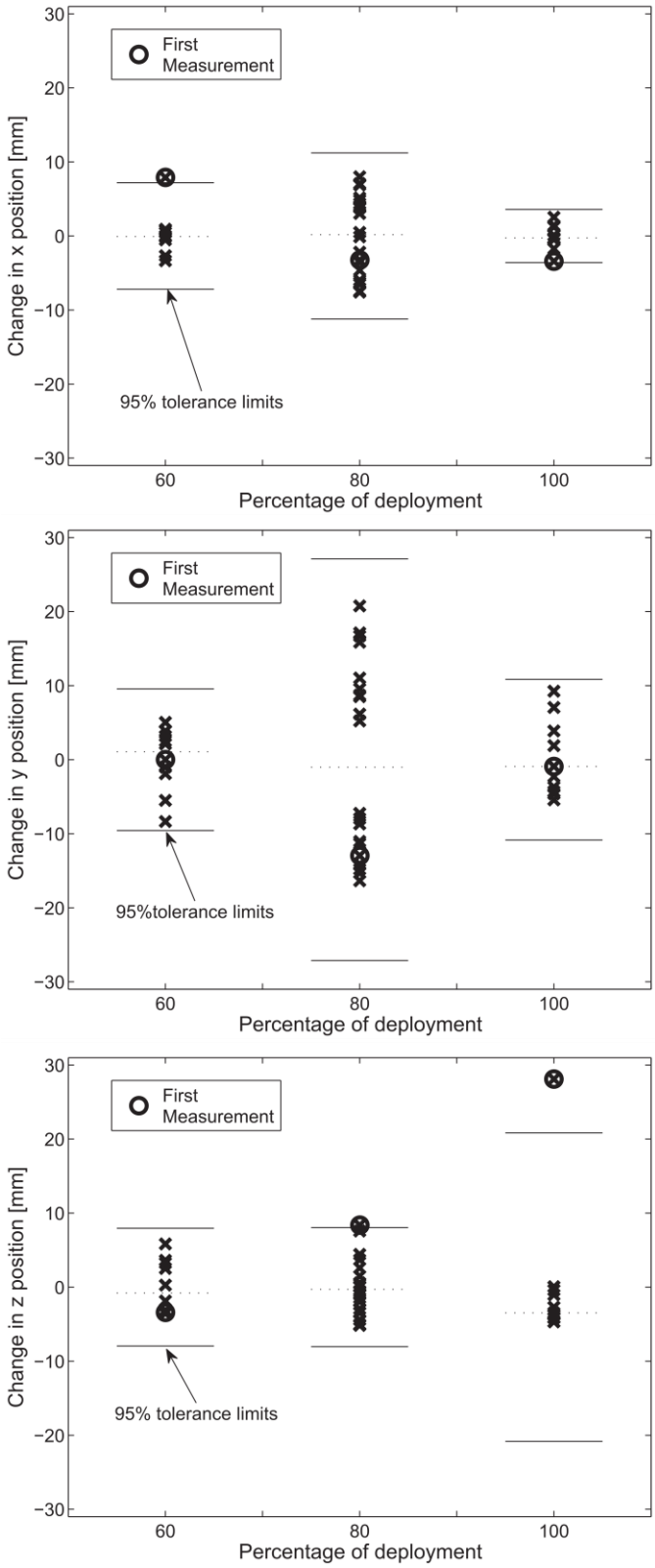

Figure 6: Relative change of positions for Node 4 over 10 cycles of folding and deployment.

Each cross in the vertical axis is the difference between the mean position over 10 cycles and the value in each cycle. The two outer lines are placed at ± two standard deviations. With the assumption of a t-distribution (distribution law for a finite sample of a population following a normal distribution), approximately 95% of values are inside the two outer lines. The standard deviations are computed separately for each axis and percentage of deployment.

There is significant variability for small length changes of active cables. Deployment positions cannot be repeated through similar length changes of active cables since the position of Node 4 changes when the same control commands are applied. Such variation is most likely due to the variable effects of friction at the joints. The first measurement has, for each deployment stage, at least one position in the three directions (x, y and z) that is more extreme than all other measurement values. This difference can be due to the setting of the structure at 100% deployment. In order to set the structure at 100% of deployment, unequal length changes of active cables had to be applied. The friction effect due to these length changes results in a variability that is more than those obtained with equal length changes during the other tests. Furthermore, joint movement suffers more friction for the first deployment phase. This behavior is therefore representative of a footbridge that remained folded for a period of time.

Table 1 shows the maximum differences from mean position values. The largest difference is observed at full deployment state. These values are only for one half of the footbridge. Assuming the same variability from the other half, the difference between the positions of two connecting nodes could be double in the worst case. At full scale, these numbers would be four times greater. This justifies the implementation of active control for connection of both halves.

Table 1: Maximum difference from mean position values for three deployment states

Percent deployment	Maximum difference [mm]
State 1 – 60%	9
State 2 – 80%	22
State 3 – 100%	28

Table 2 is a comparison between numerical analyses and laboratory test results. Numerical analyses (DR) are performed with design stresses and measured cable loads. The length increases of all active cables are 100 mm. For the numerical analyses, this length increase of active cables is divided into ten steps of 10 mm. Table 2 shows movements of front nodes are almost equal when they are calculated through numerical analysis using design and experimental inputs. Table 2 shows that the position changes for the measurement is less than the numerical analyses. This is likely due to the influence of joint friction. Unequal position changes of front nodes influence the deployment of the structure. It is concluded that structural behavior cannot be modelled satisfactorily using the assumption of dimensionless friction-free joints.

Table 2: Nodal position change of front nodes along the x axis for a 100 [mm] simultaneous length increase of all active cables.

Node	Assessment type	Nodal position change [mm]
1	DR, design stresses	105
	DR, measured cable loads	91
	Measurement	79
2	DR, design stresses	100
	DR, measured cable loads	100
	Measurement	-
3	DR, design stresses	104
	DR, measured cable loads	111
	Measurement	90
4	DR, design stresses	102
	DR, measured cable loads	94
	Measurement	84
5	DR, design stresses	103
	DR, measured cable loads	82
	Measurement	66

Table 3 shows the influence of single active cable actuation on position changes along the x axis of front nodes. The bold numbers in Table 3 refer to the position changes of nodes due to lengthening of active cables that are attached to them. Since the bold numbers are different, nodes do not move equally when their closest active cable is actuated. This is likely due to the effect of dead load on element movement. Position changes due to lengthening of all active cables simultaneously (Table 2) and those with one at a time for all active cables ("Superposition" column of Table 3) are not equal. The relative difference between the position change due to simultaneous length increase of the 5 active cables and the summation of position change for single cable length increase is shown in the last column of Table 3. Since this error is up to 113% superposition of control commands is unsuccessful. Therefore, deployment behavior is non-linearly dependent on control commands.

Table 3: Nodal position change along the x axis for a 100 [mm] single cable length increase

Node	Assessment type	Nodal position change [mm]						Relative difference %
		Cable 1	Cable 2	Cable 3	Cable 4	Cable 5	Super-position	
1	DR, design stresses	**75**	21	23	1	-44	76	38
	DR, measured cable loads	**39**	31	48	-1	-49	68	34
	Measurement	**41**	6	17	11	-30	44	80
2	DR, design stresses	-38	**60**	15	22	-9	49	104
	DR, measured cable loads	-42	**56**	31	8	-6	47	113
	Measurement	-29	**16**	25	23	1	36	-
3	DR, design stresses	-7	-25	**39**	14	34	55	89
	DR, measured cable loads	-1	-15	**42**	5	31	63	76
	Measurement	-7	0	**28**	19	15	22	64
4	DR, design stresses	30	-4	-19	**41**	28	76	34
	DR, measured cable loads	22	15	-9	**8**	26	61	54
	Measurement	10	5	2	**30**	19	66	27
5	DR, design stresses	26	25	1	-20	**70**	102	1
	DR, measured cable loads	27	33	12	-4	**24**	91	-10
	Measurement	18	-3	8	0	**12**	34	94

Two control command sequences for deployment are provided in Tables 4 and 5. The length changes of active cables for various lengths of structure are shown. The last row is the total length changes of active cables. Variability of control commands means that the paths between folded and deployed positions are not unique. Although the difference between the structural length (average position of front nodes along the x axis) at the end of sequence 1 and 2 is 8 mm, the cable length changes in sequence 1 differ from sequence 2. Thus control command sequences for deployment could be computed to minimize the length change of active cables in order to achieve the most control robustness for the in-service position.

Table 4: Length changes (mm) of active cables during stages of control command sequence 1

ΔL_{cable1}	ΔL_{cable2}	ΔL_{cable3}	ΔL_{cable4}	ΔL_{cable5}	Structure length [mm]
0	0	0	0	0	406
25	50	50	0	0	416
50	150	100	50	50	566
100	0	0	50	150	746
100	50	150	50	100	911
50	100	150	50	50	1031
50	100	0	150	0	1153
50	100	150	50	50	1253
150	100	100	100	100	1405
226	226	0	125	125	1556
251	251	251	251	251	1819
376	376	376	376	376	2113
∑=1428	∑=1503	∑=1327	∑=1252	∑=1252	

Table 5: Length changes [mm] of active cables during stages of control command sequence 2

ΔL_{cable1}	ΔL_{cable2}	ΔL_{cable3}	ΔL_{cable4}	ΔL_{cable5}	Structure length [mm]
0	0	0	0	0	426
150	100	100	150	75	681
100	100	0	100	100	828
50	201	201	0	0	999
150	50	50	50	150	1127
0	0	251	251	0	1246
0	301	0	0	0	1321
201	50	50	0	251	1465
100	50	0	100	125	1547
251	251	251	251	251	1810
376	376	376	376	376	2105
∑=1378	∑=1479	∑=1279	∑=1278	∑=1328	

Figure 7 shows the position of node 3 along y and z axes for the previous control command sequences (sequences 1 and 2). Although their positions along the deployment path are different, they reach approximately the same position at the end of deployment. Tables 4 and 5 show that the compact configuration has a length of approximately 400 mm.

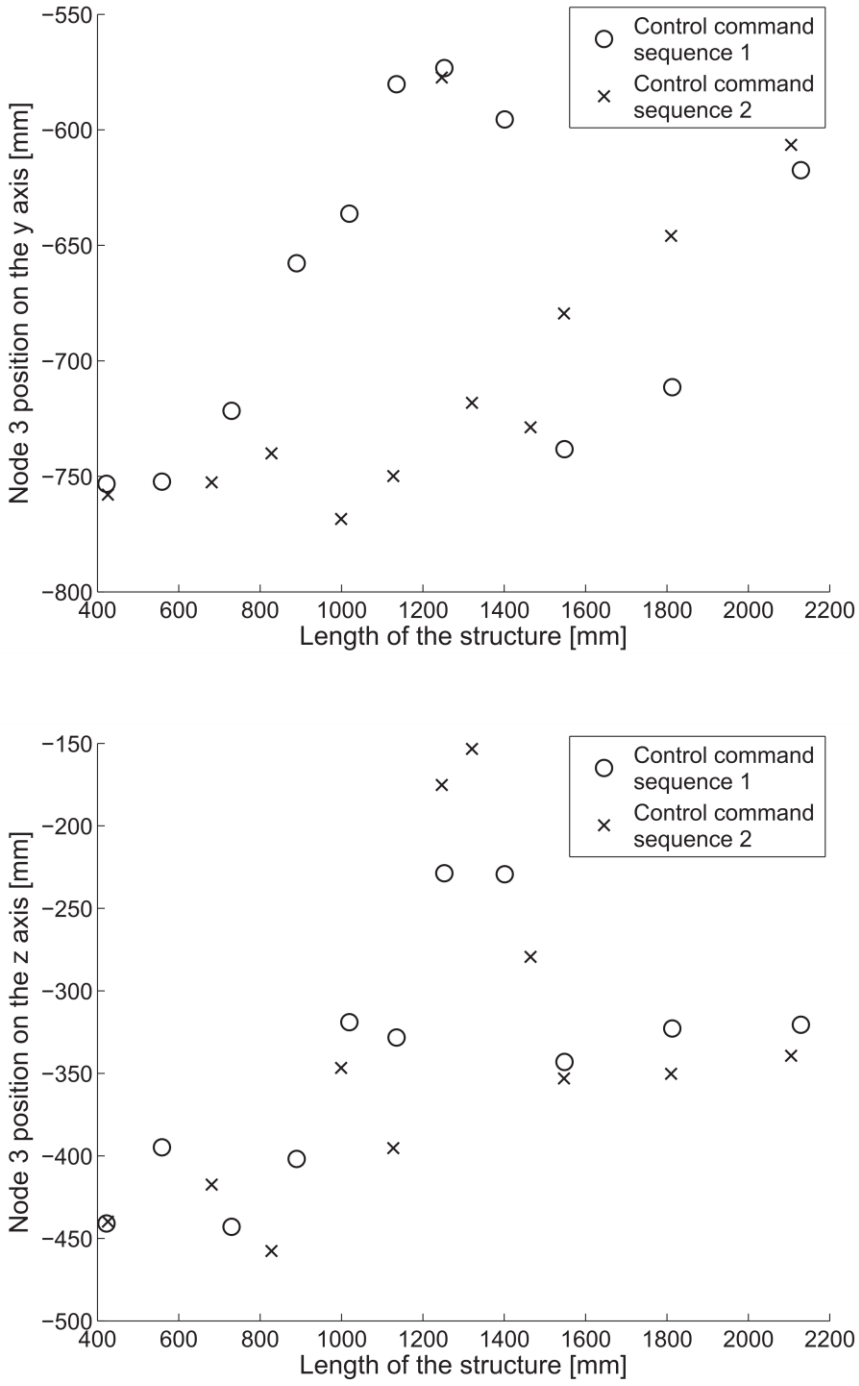

Figure 7: Positions of node 3 during deployment for control command sequence 1 and 2

Rhode-Barbarigos et al. (2012a) studied contact free-deployment path of single-module hollow-rope system. They showed that many deployment paths leading to various cable-length changes are possible. Results presented in Tables 4 and 5 support these conclusions through experimental testing.

Numerical analyses assuming dimensionless joints, as described by results in Tables 4 and 5, cannot reproduce test results. Modelling the geometry and behavior of joints is necessary. Furthermore, since during deployment, struts slide on each other, this effect needs to be modelled in numerical simulations. Figure 8 gives snapshots of deployment of the near-full-scale footbridge.

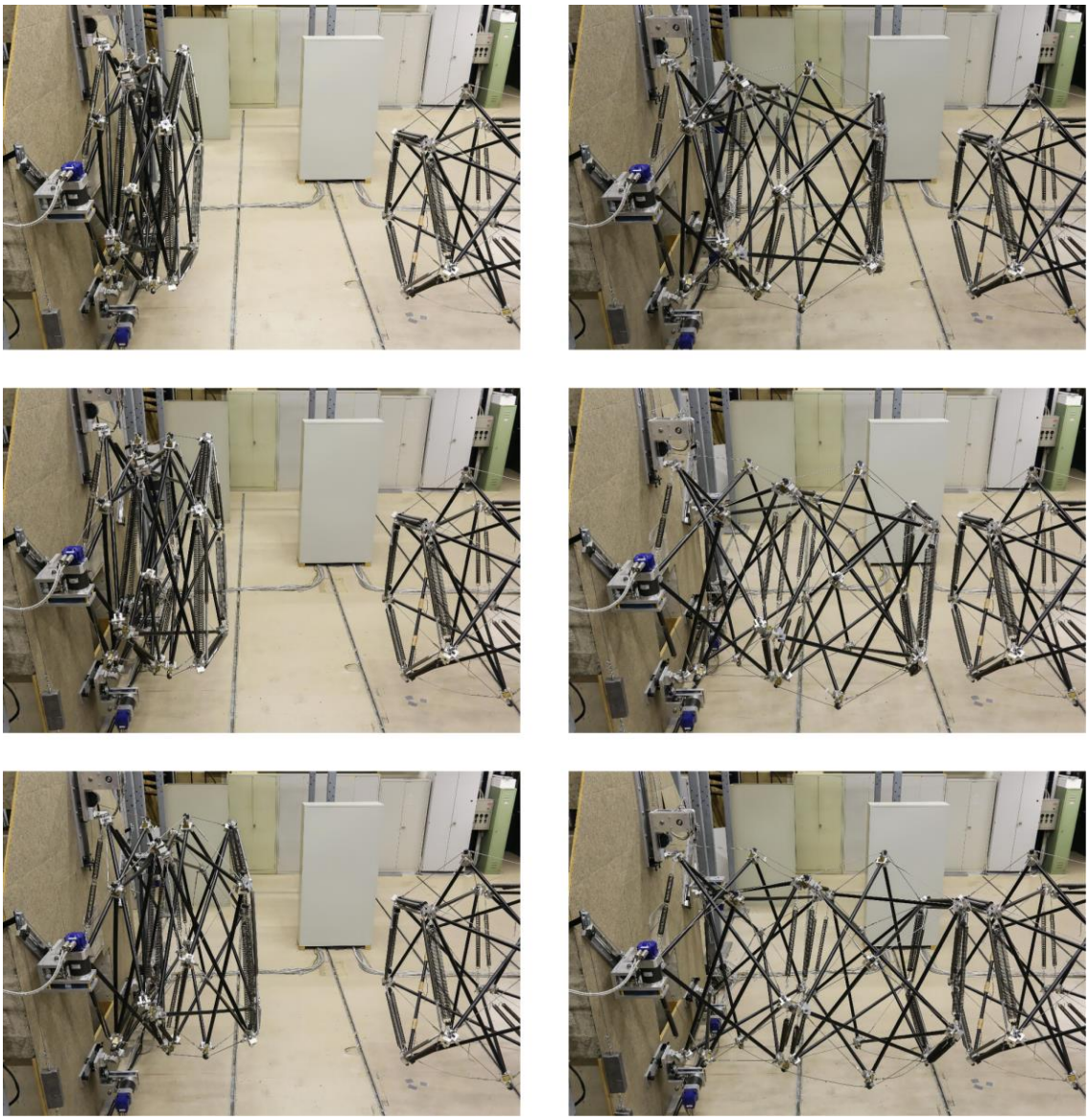

Figure 8: Snapshots of the deployment motion of the near-full-scale active deployable of one half of the tensegrity footbridge

Joints are important components of tensegrity footbridge and they significantly influence the behavior of the structure. Struts in tensegrity structures are intended to sustain compressive loading. Eccentricities at joints alter the forces through introducing bending in the struts. Although much effort has been devoted to reducing eccentricities for service at full deployment, struts are subjected to increased bending during folding. Figure 9 shows the bending of a strut due to eccentricities at joints when the footbridge is folded. This was not observed during an earlier study at 1/10 scale (Rhode-Barbarigos, et al. 2012a). Such phenomena can only be observed when near-full-scale structures are studied.

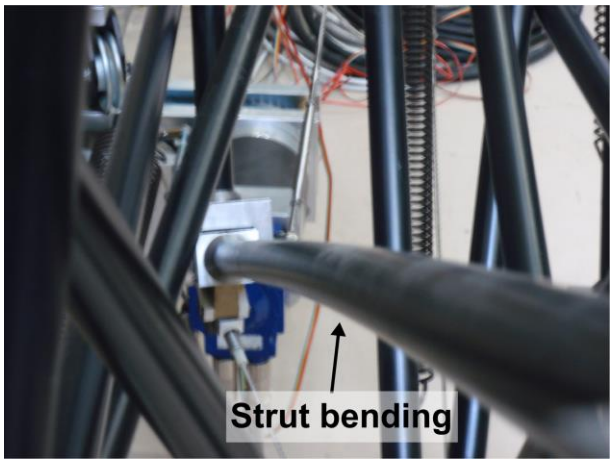

Figure 9: Bending of a strut due to joint eccentricities when the structure is folded. Bending was not observed during an earlier study of a structure at 1/10 scale.

Discussion

The deployment of one half of a tensegrity footbridge was studied both numerically and experimentally. It was shown that integration of clustered-cables and springs provides a feasible configuration for a deployable tensegrity footbridge. The control commands for deployment are actuation steps in terms of length changes of active cables. Therefore a deployment path was created through a series of equilibrium configurations. The number of actuation steps is an important parameter since large actuation steps may lead to strut contact while small actuation steps lead to an increase in deployment time.

This study has revealed several challenges for further work and these are discussed briefly below. The deployment paths caused by control command sequences are not unique. Therefore, it is important to find control command sequences having minimum length changes of active cables in order to provide flexibility when active control is needed in service.

Although continuous cables reduce number of actuators, they provide only partial control over element positions and subsequent deployment. Additionally, when active cables are slack during deployment, there is reduced control over their connected nodes. This could be avoided through calculating control commands using an additional criterion of active-cable tension. The relation

between time rate of elongation and stress of members should also be investigated for the case of continuous cables. This was investigated for a self-stress system without continuous cables and external loads (Micheletti and Williams 2007).

Springs are placed in locations so that they lengthen during folding, thereby assisting deployment as they shorten. In this study, there was no control over the length of springs during deployment and springs contain little force at the end of deployment. In further testing, the initial conditions of the structure will be modified to ensure that springs retain a minimum force at the end of deployment.

Joints influence behavior during deployment. In further work, joint movement that modifies deployment will be restricted as much as possible. The current joint design, allows for too much movement and further numerical and experimental work will reveal opportunities for modifying the degrees of freedom in selected joints.

Conclusions

- Experimental testing demonstrates that a continuous cable and spring configuration is feasible for deployment of tensegrity footbridge. Deployability of the system is aided by energy stored in springs.
- Since pre-defined control commands are unsuccessful for achieving desired deployment positions, active control is required for correction of deployment paths.
- The deployment behavior of this structure is non-linear with respect to cable length changes and therefore nodal displacements due to control commands cannot be deducted from simple superposition calculations.
- Accurate prediction of deployment requires more sophisticated analytical models than those having friction-free dimensionless joints. Also, numerical models should include the influence of strut contact, since contact free deployment paths under self-weight have not been found.
- Parameters that govern deployment include self-weight and topology. Spring stiffness also influences deployment behavior.

It is expected that tests on structures of similar complexity would reveal similar conclusions. The methodologies for determining the need for active control, non-linear analysis and explicit joint dimension modelling are likely to be applicable to other topologies of structures and other control schemes.

Acknowledgements

Authors would like to thank the Swiss National Science Foundation for supporting this work through contact number 200020_144305. This work is a continuation of a study that was initiated in collaboration with Professor René Motro, University of Montpellier, France. We thank S. D. Guest for discussions related to spring elements. Finally, we thank Patrice Gallay, Charles Gilliard and Alain Herzog for their contributions.

References

Adam, B., and Smith, I. F. C. (2008). "Reinforcement learning for structural control." Journal of Computing in Civil Engineering, 22(2), 133-139.

Argyris, J.H., and Scharpf, D.W. (1972). "Large deflection analysis of prestressed networks." ASCE Journal of the Structural Division, 98(3), 633–654.

Ashwear, N., and Eriksson, A. (2014). "Natural frequencies describe the pre-stress in tensegrity structures". Computers and Structures, 138(1), 162-171

Barnes, M.R. (1999). "Form finding and analysis of tension Structures by dynamic relaxation." International Journal of Space Structures, 14(2), 89-104.

Bel Hadj Ali, N., Rhode-Barbarigos, L., and Smith I.F.C. (2010). "Design optimization and dynamic analysis of a tensegrity based footbridge." Engineering Structures, 32(11), 3650-3659.

Bel Hadj Ali, N., Rhode-Barbarigos, L., and Smith I.F.C. (2011). "Analysis of clustered tensegrity structures using a modified dynamic relaxation algorithm." International Journal of Solids and Structures, 48(5), 637-647.

Cevaer, F., Quirant, J., and Dubé, J.-F. (2011). "Mechanical behaviour in compression of a foldable tensegrity ring: parametric study and rheological model." International Journal of Space Structures, 27(2), 107-115.

Domer, D. (2003). "Performance enhancement of active structures during service lives." PhD Thesis No. 2750, Ecole Polytechnique Fédérale de Lausanne (EPFL), Lausanne, Switzerland.

Domer, B., and Smith, I. F. C. (2005). "An active structure that learns." Journal of Computing in Civil Engineering, 19(1), 16-24.

Dalil Safaei, S., Eriksson, A., Micheletti, A., and Tibert, G. (2013). "Study of various tensegrity modules as building blocks for slender booms." International Journal of Space Structures, 28(1), 41-52.

Fest, E., Shea, K., and Smith, I. F. C. (2004). "Active tensegrity structure." Journal of Structural Engineering, 130(10), 1454-1465.

Furuya, H. (1992). "Concept of deployable tensegrity structures in space applications", International Journal of Space Structures, 7(2), 143-151.

Furuya, H., Nakahara, M., Murata, S., Jodoi, D., Terada, Y., and Takadama, K. (2006). "Concept of inflatable tensegrity for large space structures." Structural Dynamics and Materials Conference., Collection of Technical Papers - AIAA/ASME/ASCE/AHS/ASC Structures, American Institute of Aeronautics and Astronautics, Reston, VA, 1322-1330.

Guest, S.D. (2006). "The stiffness of prestressed frameworks: a unifying approach." International Journal of Solids and Structures. 43(3-4), 842-854.

Michelleti, A. and Williams, W.O., (2007).”A marching procedure for form-finding for tensegrity structures.” Journal of Mechanics of Materials and Structures, 2(5), 857-882.

Moored, K.W. and Bart-Smith H. (2009). “Investigation of clustered actuation in tensegrity structures.” International Journal of Solids and Structures, 46(17), 3272-3281.

Murakami, H. (2001). “Static and dynamic analyses of tensegrity structures. Part I. Nonlinear equations of motion.” International Journal of Solids and Structures, 38(20), 3599–3613.

Motro, R., Maurin, B., and Silvestri, C. (2006). “Tensegrity Rings and the Hollow Rope.” IASS Symposium, New Olympics, New Shells and Spatial Structures, International Association for Shell and Spatial Structures, Madrid, Spain, 470-471.

Motro, R. and Raducanu, W. (2003). “Tensegrity Systems.”, International Journal of Space Structures, 18(2), 77-84.

Nguyen, A.D., Quirant, J., Cevaer, F., Dubé, J.-F. (2011). “Study and construction of a pentagon-based tensegrity ring.” European Journal of Environmental and Civil Engineering, 15(6), 849-868.

Pellegrino, S. and Calladine, C.R. (1986). “Matrix analysis of statically and kinematically indeterminate frameworks.” International Journal of Solids and Structures, 22(4), 409-428.

Pugh, A., (1976). “An Introduction to Tensegrity.” University of California Press, Berkley, CA.

Rhode-Barbarigos, L., Bel Hadj Ali, N., and Smith, I.F.C. (2010). “Designing tensegrity modules for pedestrian bridges.” Engineering Structures, 32(4). 1158-1167.

Rhode-Barbarigos. L., Schulin. C., Bel Hadj Ali, N., Motro, R., and Smith I.F.C. (2012a). “Mechanism-based approach for the deployment of a tensegrity-ring module.” Journal of Structural Engineering-ASCE, 138, 539-548.

Rhode-Barbarigos, L., Bel Hadj Ali, N., Motro, R., and Smith I.F.C. (2012b). “Design aspects of a deployable tensegrity-hollow-rope footbridge.” International Journal of Space Structures, 27(2), 81-96.

Schenk, M., Guest, S.D., Herder, J.L. (2007). “Zero stiffness tensegrity structures.” International Journal of Solids and Structures, 44(20), 6569-6583.

Skelton, R. E., Adhikari, R., Pinaud, J., Chan, W., and Helton, J. W. (2001). “An introduction to the mechanics of tensegrity structures.” Proceedings of the IEEE Conference on Decision and Control, IEEE, Piscataway, NJ, 4254-4259

Skelton, R. E., Fraternali, F., Carpentieri, G., and Micheletti, A. (2014). ”Minimum mass design of tensegrity bridges with parametric architecture and multiscale complexity.” Mechanics Research Communications, 58, 124-132.

Tibert, G. (2002). “Deployable tensegrity structures for space applications.” PhD thesis, Royal Institute of Technology, Stockholm, Sweden.

Tibert, A. G. and Pellegrino, S. (2003). "Review of form-finding methods for tensegrity structures." International Journal of Space Structures, 18 (4), 209–223.

Zolesi, V. S., Ganga, P. L., Scolamiero, L., Micheletti, A., Podio-Guidugli, P., Tibert, G., and Ghiozzi, M. (2012). "On an innovative deployment concept for large space structures." Proceedings of 42nd International Conference on Environmental Systems, San Diego, California, USA.